

Density of states and temperature dependence of the exponent in the light-intensity behavior of *a*-Si:H photoconductivity

D. Mendoza and W. Pickin

Instituto de Investigaciones en Materiales, Universidad Nacional Autónoma de México, Apartado Postal 70-360, México, Distrito Federal 04510, México

(Received 3 November 1988; revised manuscript received 26 April 1989)

We report experimental measurements concerning the temperature dependence of the γ exponent in the light-intensity behavior of the photoconductivity of hydrogenated amorphous silicon (*a*-Si:H). We find that good agreement between experimental results and numerical calculations is achieved if a peak in the density of states (DOS) above the dark Fermi level is assumed. Other forms suggested for the DOS in *a*-Si:H are surveyed for comparison. Finally, we propose a simple relation between DOS and measurable quantities and make estimates for some physical parameters for this material.

INTRODUCTION

Transient photoconductivity as well as steady-state photoconductivity techniques have been used to obtain information about the recombination of carriers with localized states in the gap, as well as the energy distribution of those states. Experimentally, for a wide range of temperatures and light intensities, the photoconductivity σ_{ph} is proportional to I^γ , where I is the light intensity and γ a quantity dependent on temperature and light intensity.¹⁻³

A good deal of theoretical work has been devoted to this subject in order to explain the σ_{ph} versus $1/T$ and σ_{ph} versus I behavior in amorphous semiconductors.^{4,5} However, little attention has been paid to the temperature dependence of the exponent γ . Rose⁶ was the first to obtain an explicit form of the γ dependence with the temperature for some semiconductors. By modeling the trap distribution with an exponential function of the energy in the form $g(E) = g_c \exp[-(E_c - E)/E_1]$ he found

$$\gamma = E_1 / (E_1 + kT). \quad (1)$$

In the case of hydrogenated amorphous silicon (*a*-Si:H) the applicability of this result is not obvious. For example, Bhattacharya and Narasimhan⁷ carried out numerical calculations and found the same temperature dependence of γ as Rose's result for different forms of density of states. They concluded that neither the intensity dependence of photoconductivity nor the temperature dependence of the exponent may be used as evidence for an exponential gap-state distribution.

Other authors^{8,9} have obtained results similar to Rose's by modeling the conduction-band tail with an exponential function, and other simple γ - T relations depending on the approximations and the model used in their calculations. A serious problem is that the experimental results on the temperature dependence of γ reported in the present work and by other authors⁷ cannot be explained by Rose's result. Nevertheless, many authors (see, for example, Refs. 2, 3, and 10) use Rose's work to explain their experimental results.

The aim of the present work is to present simple (but complete) numerical calculations that satisfactorily explain our experimental results of the γ dependence on temperature for undoped *a*-Si:H as well as a simple expression relating density of states and measurable quantities.

EXPERIMENTAL DETAILS

Undoped amorphous silicon films were deposited onto Corning 7059 glass substrates by rf glow-discharge decomposition of silane. The characteristics of the two samples used in the present work are as follows. Sample 1 (sample 2): silane pressure equal to 500 mTorr (150 mTorr), substrate temperature of 255°C (240°C), power dissipation of 146 mW/cm² (86 mW/cm²), sample thickness of 3.6 μ m (1 μ m), and dark activation energy equal to 0.81 eV (0.79 eV). Good Ohmic aluminum contacts of 1 cm length and 0.5-mm spacing were deposited by evaporation.

Illumination was supplied by a tungsten lamp with a red filter centered at 620 nm. Light intensity varied from 10¹¹ to 10¹⁴ photons/cm²s. With this intensity of light we are sure that the Staebler-Wronski effect never happened in the sample.¹¹ The sample was introduced into a vacuum chamber ($P \sim 8 \times 10^{-6}$ Torr) and the temperature was varied from 200 to 400 K. Prior to each experiment the sample was annealed for 30 min at 200°C and 8×10^{-6} Torr. With a voltage bias of 50 V the photocurrent was measured with an electrometer (Keithley 619) and then the value of γ was extracted from a photocurrent versus light intensity plot for each temperature. We should note that at higher light intensities than those reported in the present work a curvature appears in the plot of $\log(I)$ versus $\log(\sigma_{ph})$. To avoid this curvature, we worked in the low-light-intensity region.

MODEL

The fractional occupation $f(E)$ of gap states of energy E is

$$f = nb_n / (nb_n + a_n) . \quad (2)$$

Here n is the electron concentration, a_n is the transition rate from gap states to the conduction band, and b_n is a trapping coefficient. In this model we suppose⁸ $a_n = a_{nt} + a_{no}$, where $a_{nt} = N_C b_n \exp[-(E_c - E)/kT]$ is the thermal excitation rate [$N_C = kTg(E_c)$], and a_{no} is the optical transition rate, which we assumed to be proportional to the light intensity I in the form $a_{no} = \sigma^* I$ with σ^* the optical cross section. The neutrality condition is

$$(n - n_0) + \int_{E_F}^{E_c} f(E)g(E)dE = \int_{E_v}^{E_F} [1 - f(E)]g(E)dE , \quad (3)$$

where n_0 is the dark value of n and $g(E)$ is the density of states. In amorphous semiconductors the trapped concentration will normally exceed the free concentration and the term $n - n_0$ can be neglected. Equation (3) becomes

$$\int_{E_F}^{E_c} \frac{nb_n g(E)}{nb_n + a_{nt} + a_{no}} dE = \int_{E_v}^{E_F} \frac{a_{no} g(E)}{nb_n + a_{no}} dE , \quad (4)$$

where a_{nt} is neglected for $E < E_F$. We suppose that b_n is independent of energy and takes the value found in transient experiments¹² of $\sim 4 \times 10^{-8} \text{ cm}^3 \text{ s}^{-1}$. Finally, we assume that a_{no} is independent of the energy.

After rearranging Eq. (4) becomes

$$nb_n (1 + nb_n / a_{no}) \int_{E_F}^{E_c} \frac{g(E)}{nb_n + a_{nt} + a_{no}} dE = \int_{E_v}^{E_F} g(E) dE = \text{const} \equiv K . \quad (5)$$

Supposing a specific model of the density of states $g(E)$, we plot $\log(a_{no})$ versus $\log(n)$ and compute the slope (γ) for various temperatures. The values of a_{no} were selected in order to make n_0 negligible compared with n , and, from this point, a_{no} was varied 4 orders of magnitude upwards. Typically, a_{no} varied from 10^{-4} to 1 s^{-1} ; the upper limit in a_{no} was chosen to avoid the curvature in the $\log(a_{no})$ versus $\log(n)$ graph. This kind of curvature has been found experimentally in $a\text{-Si:H}$ for high light intensities.¹¹ Using the optical cross-section value found in the present work of $\sim 10^{-14} \text{ cm}^2$, the equivalent values of the light intensities are from 10^{10} to $10^{14} \text{ photons/cm}^2 \text{ s}$, which are much less than $\sim 3 \times 10^{17} \text{ photons/cm}^2 \text{ s}$ (100 mW/cm^2 of red light) used as a minimum light intensity to produce the Staebler-Wronski effect.¹¹

Note that details in the form of $g(E)$ below E_F are irrelevant in the present model [see Eq. (5)] and the value of the constant K will generally depend on the form of $g(E)$ near the valence-band edge. For instance, if we model $g(E)$ near E_v as $g(E_v) \exp(-E/E_2)$ then $K \approx E_2 g(E_v)$. On the other hand, in order to obtain an explicit expression for the density of states, we use the relation

$$G = b_r n \int_{E_F}^{E_c} f(E)g(E)dE , \quad (6)$$

where G is the optical generation rate and b_r is a recom-

bination coefficient. Expression (6) is valid if recombination is dominated by carriers in transport states.⁸ At low light intensities—which is the case in the present work—and not very high temperatures, the distribution function $f(E)$ is given by Eq. (2) cut off at the quasi-Fermi-level E_{Fn} given by

$$E_{Fn} = E_c - kT \ln(N_c / n) , \quad (7)$$

hence, the upper limit in Eq. (6) can be approximated by E_{Fn} . If we suppose $n \sim G^\gamma$ then $d[\ln(n)]/d[\ln(G)] = \gamma$. Extracting this logarithmic derivative from Eq. (6) at constant temperature we have finally

$$g(E_{Fn}) \approx \frac{2}{3} (G / b_r n) [(\gamma^{-1} - 1) / kT] . \quad (8)$$

As $G = \alpha \eta I$, where α is the absorption coefficient and η the quantum efficiency, then Eq. (8) becomes

$$g(E_{Fn}) \approx g_0 (a_{no} / n) [(\gamma^{-1} - 1) / kT] , \quad (9)$$

where $g_0 = 2\alpha\eta / 3\sigma^* b_r$. Note that the validity of relation (8) is limited by the approximation of the upper limit in the integral of Eq. (6).

We worked three different models of the gap density of states (DOS) frequently used in the literature for $a\text{-Si:H}$, namely the following.

(a) Exponential band tails and a Gaussian distribution in the middle of the gap (see, for example, Ref. 13),

$$g_a(E) = g_3 \exp(-E/E_3) + g_2 \exp[-(E - E_4)^2 / E_2^2] + g_1 \exp[-(E_c - E)/E_1] , \quad (10)$$

where $g_1 = g_3 = 10^{21} \text{ eV}^{-1} \text{ cm}^{-3}$, $g_2 = 10^{17} \text{ eV}^{-1} \text{ cm}^{-3}$, $E_1 = 25 \text{ meV}$, $E_2 = 140 \text{ meV}$, $E_3 = 45 \text{ meV}$, and $E_4 = 0.8 \text{ eV}$. In this work the zero in energy was taken at the valence-band edge, i.e., $E_v = 0 \text{ eV}$ and $E_c = 1.8 \text{ eV}$.

(b) Exponential valence tail, Gaussian distribution in the middle of the gap, and Gaussian distribution for the conduction tail,

$$g_b(E) = g_3 \exp(-E/E_3) + g_2 \exp[-(E - E_4)^2 / E_2^2] + g_1 \exp[-(E_c - E)^2 / E_1^2] , \quad (11)$$

where all the parameters are the same as in model (a), although in this case we worked with two values for E_1 : 65 and 100 meV. The Gaussian form for the DOS near E_c has been used in Ref. 7.

(c) Exponential band tails and two Gaussian distributions in the middle of the gap,^{14,15}

$$g_c(E) = g_3 \exp(-E/E_3) + g_2 \exp[-(E - E_4)^2 / E_2^2] + g_2 \exp[-(E - E_5)^2 / E_2^2] + g_1 \exp[-(E_c - E)/E_1] , \quad (12)$$

where all the parameters take the same values as before, except the following: $E_1 = 25 \text{ meV}$, $E_3 = 50 \text{ meV}$, $E_4 = 0.8 \text{ eV}$, $E_5 = 1.2 \text{ eV}$, and two cases for E_2 ($E_2 = 60$ and 100 meV). In all the situations the dark Fermi level was taken 1 eV from the valence-band edge.

RESULTS AND DISCUSSION

Figure 1 displays the experimental results of γ^{-1} against T for the two samples used in the present work [dots (sample 1) and crosses (sample 2)]. We first note that these results cannot be explained with Rose's result (dashed line). The solid line corresponds to calculations based on model (c) described above for the DOS with $E_2 = 60$ meV [see Eq. (12)].

In Fig. 2 we show the behavior of γ^{-1} versus T for model (a) given by Eq. (10). In the inset, a graph of the DOS is shown. We note that Eq. (1) is obtained as an asymptotic approximation at low temperatures (dashed line). Also shown in the inset is a solid line which shows the region in the DOS swept by E_{Fn} when the light intensity is varied by 4 orders of magnitude at a fixed temperature. The conversion into an energy scale is done by using the definition of the quasi-Fermi-level E_{Fn} [Eq. (7)].

From Fig. 2 it is clear that, in the low-temperature region, E_{Fn} moves in the exponential band tail and then γ behaves as Eq. (1); but in the high-temperature region the result obtained with our model differs from Rose's result (dashed line) because E_{Fn} moves in a region of the DOS which is not a simple exponential. With this model of DOS we cannot reproduce the experimental results (see Fig. 1).

In Fig. 3 the behavior of the temperature dependence of γ^{-1} is shown when we model the DOS by $g_b(E)$ represented by Eq. (11) with $E_1 = 65$ meV (curve A) and $E_1 = 100$ meV (curve B), as shown in the inset. Again, the solid line in the DOS represents the region in which E_{Fn} moves at fixed temperature and changing light intensity.

An important feature of that result is that when the conduction tail is modeled by a Gaussian distribution we cannot obtain a Rose-type behavior; i.e., the results

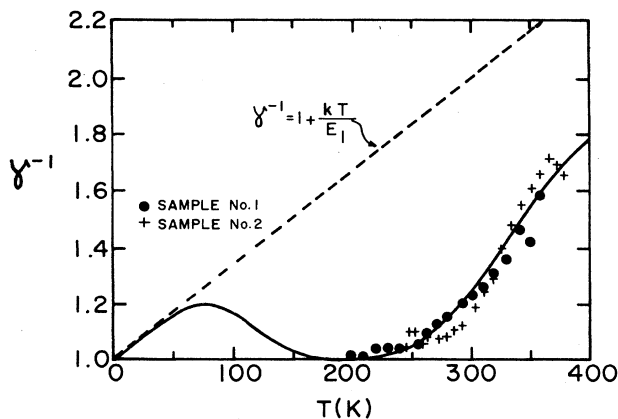


FIG. 1. Graph for experimental values of γ^{-1} vs T . Dots (sample 1), crosses (sample 2), and theoretical calculations (solid line) assuming a Gaussian peak in the density of states centered at 1.2 eV above the valence-band edge and a width of 60 meV. Dashed line corresponds to the Rose-type approximation.

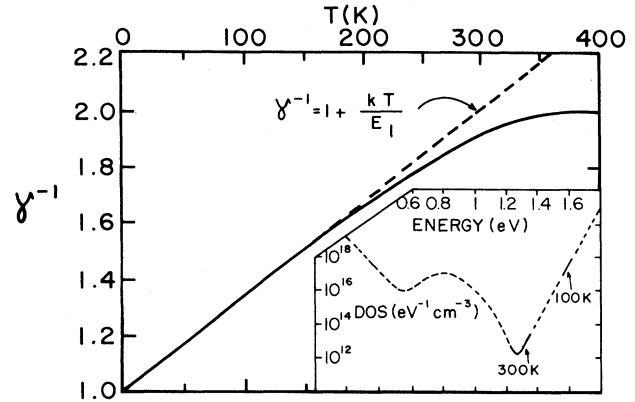


FIG. 2. Numerical calculations of γ^{-1} vs T using the density of states that is shown in the inset; the dashed line corresponds to Rose's result. The solid line in the density of states corresponds to the region where the quasi-Fermi-level moves at the shown temperature.

shown in Fig. 3 cannot be approximated in any region by $\gamma^{-1} = 1 + kT/E_1$. We should note that this result is opposed to Bhattacharya and Narasimhan's numerical prediction.⁷ Again, with this model of the DOS we cannot reproduce the experimental results obtained in the present work (see Fig. 1).

In Fig. 4 we show γ^{-1} versus T when the DOS is modeled by two Gaussians in the middle of the gap [Eq. (12)] with $E_2 = 100$ meV as shown in the inset. The main features of this result are (1) at very low temperatures we recover asymptotically Eq. (1) which corresponds to the region in energy where E_{Fn} moves into the exponential conduction-band tail; (2) around room temperature, the Gaussian peak located above E_F becomes very important in the form of $\gamma(T)$; and (3) there is some similarity be-

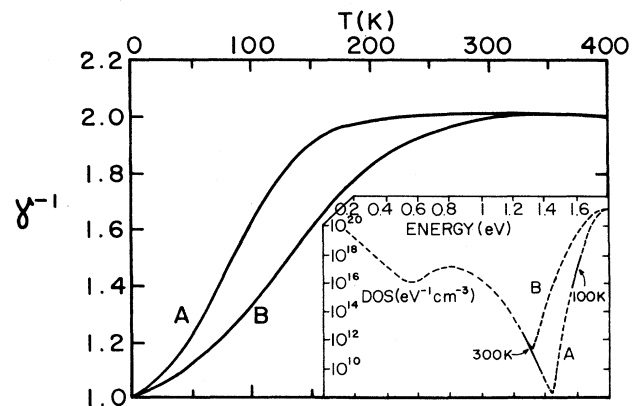


FIG. 3. Numerical calculations of γ^{-1} vs T using the density of states shown in the inset. Curves A and B correspond to a Gaussian conduction tail width of 65 and 100 meV, respectively. The solid line in the density of states corresponds to the region where the quasi-Fermi-level moves at the shown temperature.

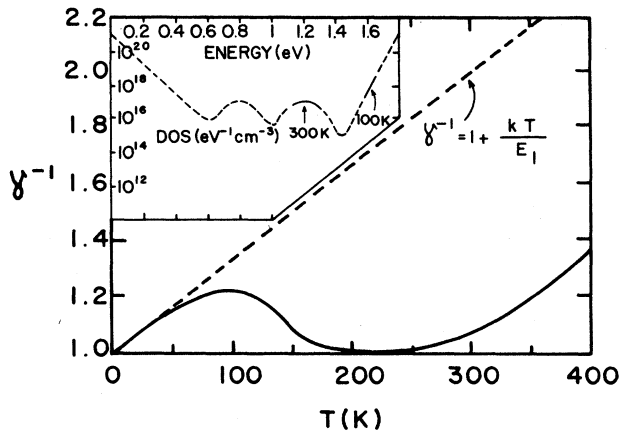


FIG. 4. Numerical calculations of γ^{-1} vs T using the density of states shown in the inset. Dashed line corresponds to the results of Rose. The solid line in the density of states corresponds to the region where the quasi-Fermi-level moves at a fixed temperature.

tween this result and the experimental form of $\gamma^{-1}(T)$. We have, therefore, worked with the Gaussian width. A good fit to the experimental results is observed when $E_2 = 60$ meV for sample 1. This result is plotted as a solid line in Fig. 1.

The peak above E_F corresponds to doubly occupied negatively charged dangling bonds which are unoccupied in intrinsic a -Si:H at $G=0$, but are highly occupied for values of $G \neq 0$.¹⁵ On the other hand, the energy location of the dangling-bond levels, neutral (D^0), and doubly occupied (D^-) dangling bonds, has been classified into two groups.¹⁶ Group *A* placed D^- at 0.8–0.9 eV and D^0 at 1.2–1.3 eV below E_c , and group *B* placed D^- at 0.5–0.65 eV and D^0 at 0.9–1.1 eV below E_c .¹⁷ In the present case we choose the energy levels of 1 eV for D^0 and 0.6 eV for D^- below E_c as in Kocka's model¹⁴ for undoped a -Si:H (group *B*). Additionally we assume an effective correlation energy of $U = 0.4$ eV (Ref. 16) and that the dark Fermi level is pinned between the D^0 and D^- levels.¹⁸

At this stage we are able to estimate some parameters. For sample 1 and using model (c) for the DOS, at $T = 300$ K the value of the optical cross section (σ^*) is obtained as follows: We select $a_{no} = 1$ s⁻¹ and solving Eq. (5) for n we obtain $n = 1.2 \times 10^{11}$ cm⁻³, using the expression for the conductivity ($\sigma = q\mu n$) with μ taken arbitrarily as 5 cm² V⁻¹ s⁻¹,¹⁹ we see that the value measured for I which corresponds to that value of the conductivity (and consequently n) is 6.8×10^{13} photons/cm² s; so the value of $\sigma^* = a_{no}/I$ is $\sim 1.4 \times 10^{-14}$ cm².

Using the equivalence between Eqs. (5) and (6) we have

$$b_r/b_n \sim \alpha\eta/K\sigma^*, \quad (13)$$

with $\alpha(2 \text{ eV}) \sim 2 \times 10^4 \text{ cm}^{-1}$,²⁰ $\sigma^* \sim 10^{-14} \text{ cm}^2$, and $K = 5 \times 10^{19} \text{ cm}^{-3}$ [here $K = E_3 g(E_v)$ with $E_3 = 50$ meV and $g(E_v) = 10^{21} \text{ eV}^{-1} \text{ cm}^{-3}$ for model (c) of the DOS],

and we have $b_r/b_n \sim 4 \times 10^{-2} \eta$ which means, as $\eta \leq 1$, that $b_r < b_n$. In the multiple trapping theory⁸ we have the weak recombination regime when $b_r < b_n$ and strong recombination regime in the opposite case. Hence the material studied in the present work falls within the weak recombination regime and it is consistent with previous experiments on transient photoconductivity.¹²

The constant g_0 in Eq. (9) takes the value $g_0 = 2K/3b_n \sim 8.3 \times 10^{26} \text{ cm}^{-6} \text{ s}$; a graph of the original density of states and $g(E)$ calculated with Eq. (9) appears in Fig. 5(a). The quantities a_{no} and n are solutions of Eq. (5), and the value of γ is extracted from these values. We note that the general form of the original $g(E)$ is reproduced but there is disagreement at low energies which correspond to high temperatures in the energy scale given by Eq. (7). Let us now make some estimates of the density of states for sample 1. At $T = 300$ K, the experimental values are $I = 6.86 \times 10^{13}$ photons/cm² s, $\sigma = 9.4 \times 10^{-8} (\Omega \text{ cm})^{-1}$, and $\gamma^{-1} = 1.2$. Now using $a_{no} = \sigma^* I$ and $n = \sigma/q\mu$ with $\mu = 5 \text{ cm}^2 \text{ V}^{-1} \text{ s}^{-1}$ and $\sigma^* \sim 10^{-14} \text{ cm}^2$ we have $a_{no} \sim 0.7 \text{ s}^{-1}$ and $n \sim 1.17 \times 10^{11} \text{ cm}^{-3}$. With these values and Eq. (7) the energy scale at $T = 300$ K is

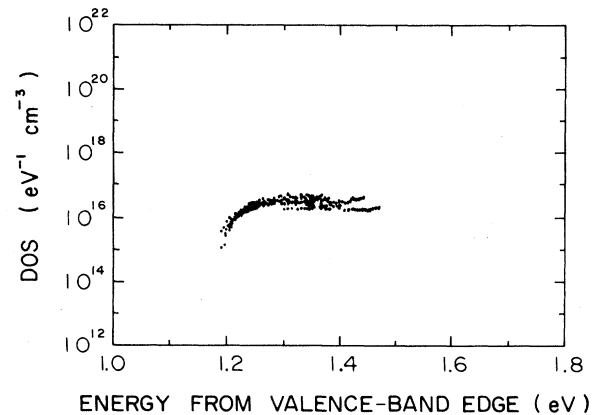
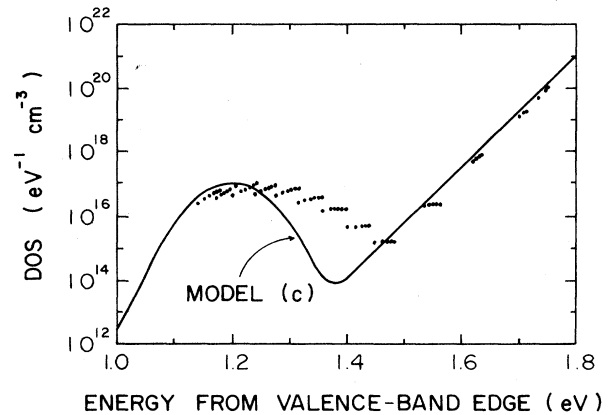


FIG. 5. (a) Original density of states (solid line) and calculated DOS using an inversion formula (dotted line). See text. (b) Gap density of states against energy for sample 1. These values were deduced using the measured quantities T , I , σ , and γ , and Eq. (9). See text.

$E_{Fn} \sim 1.32$ eV. Finally with $g_0 = 8.3 \times 10^{26} \text{ cm}^{-6} \text{ s}$ and Eq. (9) we have $g(1.32 \text{ eV}) \sim 4.2 \times 10^{16} \text{ cm}^{-3} \text{ eV}^{-1}$. Figure 5(b) shows a more complete graph of the density of states versus energy in the gap for sample 1.

CONCLUSION

Using a very simple model we are able to reproduce satisfactorily experimental results of the temperature dependence of γ . Our experimental results cannot be explained by Rose's result. However, with our model we confirm it as an asymptotic behavior at very low temperatures when the quasi-Fermi-level moves into an exponential band tail of the density of states near the conduction-band edge.

We have deduced a very simple expression for the density of states which is more accurate at low temperatures. This result can be generalized to any amorphous semiconductor.

The material studied in the present work falls within the weak recombination regime, i.e., $b_r < b_n$ and if we take the quantum efficiency as unity then $b_r \sim 1.6 \times 10^{-9} \text{ cm}^3 \text{ s}^{-1}$.

Finally, we think that in a better approximation it would be necessary to consider the energy dependence of b_n .

ACKNOWLEDGMENTS

We thank Manuel García for preparing the samples used in these experiments. We also thank Salvador Cruz for helpful comments. We acknowledge financial support from the Organization of American States and the Consejo Nacional de Ciencia y Tecnología. (CONACyT), México.

-
- ¹W. E. Spear, R. J. Loveland, and A. Al-Sharbaty, *J. Non-Cryst. Solids* **15**, 410 (1974).
²P. J. Zanzucchi, C. R. Wronski, and D. E. Carlson, *J. Appl. Phys.* **48**, 5227 (1977).
³C. Y. Huang, S. Guha, and S. J. Hudgens, *Phys. Rev. B* **27**, 7460 (1983).
⁴J. G. Simmons and G. W. Taylor, *J. Phys. C* **7**, 3051 (1974).
⁵Benyuan Gu, Daxing Han, Chenxi Li, and Shifu Zhao, *Philos. Mag.* **53**, 321 (1986).
⁶A. Rose, *Concepts in Photoconductivity and Allied Problems* (Interscience, New York, 1963).
⁷E. Bhattacharya and K. L. Narasimhan, *Phys. Rev. B* **28**, 2287 (1983).
⁸M. A. Kastner and D. Monroe, *Solar Energy Mater.* **8**, 41 (1982).
⁹V. Halpern, *J. Phys. C* **21**, 2555 (1988).
¹⁰E. Arene and J. Baixeras, *Phys. Rev. B* **30**, 2016 (1984).
¹¹C. R. Wronski, in *Semiconductors and Semimetals*, edited by J. I. Pankove (Academic, New York, 1984), Vol. 21, Part C.
¹²D. Mendoza and W. Pickin (unpublished).
¹³T. Drüsedau, D. Wegener, and R. Bindermann, *Phys. Status Solidi B* **140**, K27 (1987).
¹⁴J. Kocka, *J. Non-Cryst. Solids* **90**, 91 (1987).
¹⁵T. J. McMahon and J. P. Xi, *Phys. Rev. B* **34**, 2475 (1986).
¹⁶P. G. LeComber and W. E. Spear, *Philos. Mag. B* **53**, L1 (1986).
¹⁷K. Mori, H. Okushi, and K. Tanaka, *J. Non-Cryst. Solids* **97&98**, 723 (1987); K. L. Ngai and R. Q. Han, *Solid State Commun.* **68**, 155 (1988).
¹⁸M. Stutzmann and W. B. Jackson, *Solid State Commun.* **62**, 91 (1987).
¹⁹See, for example, P. G. LeComber, A. Madam, and W. E. Spear, *J. Non-Cryst. Solids* **11**, 219 (1972); in *Electronic and Structural Properties of Amorphous Semiconductors*, edited by P. G. LeComber and J. Mort (Academic, New York, 1973); W. E. Spear and P. G. LeComber, *Philos. Mag. B* **52**, 247 (1984).
²⁰G. D. Cody, in *Semiconductors and Semimetals*, edited by J. I. Pankove (Academic, New York, 1984), Vol. 21, Part B.